Nanowire-Based Molecular Monolayer Junctions: Synthesis, Assembly, and Electrical Characterization

L. T. Cai,[†] H. Skulason,[‡] J. G. Kushmerick,[§] S. K. Pollack,[§] J. Naciri,[§] R. Shashidhar,[§] D. L. Allara,[‡] T. E. Mallouk,[‡] and T. S. Mayer*[,†]

Department of Electrical Engineering and Department of Chemistry, The Pennsylvania State University, University Park, Pennsylvania 16802, and Center for Bio/Molecular Science and Engineering, Naval Research Laboratory, Washington, DC 20375

Received: July 21, 2003

Nanowire metal−molecule−metal junctions containing dithoilated molecules of dodecane (C12), oligo(phenylene ethynylene) (OPE), and oligo(phenylene vinylene) (OPV) were prepared by replicating the pores of sub-40 nm diameter polycarbonate track etched membranes. Bottom Au−S or Pd−S contacts were made by potential-assisted molecule assembly onto the tips of the first segment of the electrochemically deposited nanowires. Top S−Ag or S−Pd contacts were formed by depositing Ag or Pd nanoparticles, which also served as a thin seed layer for electrodeposition of the second nanowire segment. Room-temperature current−voltage (I−V) measurements of individual nanowires show that the conductance of junctions formed with π-conjugated oligomers are several orders of magnitude larger than the saturated alkanes, with the OPV junctions having the highest conductance. The molecular wire junction conductance was also found to be dependent on the metal contacts with symmetric Pd−Pd junctions yielding the best metal−molecule coupling and highest conductance.

1. Introduction

Molecular electronics promises to deliver ultrahigh-density memory and logic circuits that can be realized with dimensions well below the scaling limits of conventional top-down fabrication methods associated with silicon technology.[1] Considerable progress has been made toward this end by developing test beds to characterize the electrical transport properties of individual molecules or small assemblies of molecules. Measurements have been taken on individual molecules using scanning−tunneling probe contacts[2,3] and controllable break junctions.[4−6] These studies have revealed fundamentals related to conduction through aromatic molecular wires and switching in nitroaromatic molecules[7] as well as coulomb blockade and kondo effects in C-60.[8] Self-assembled monolayers (SAMs) of molecules have been characterized with top metal contacts formed using atomic force probes,[9−12] mercury drops,[13,14] low-temperature evaporation,[15,16] electroless deposition,[17] and crossing metal wires.[18,19] Molecular junctions fabricated with SAMs of nitroaromatics[20,21] and rotaxanes[22] have exhibited technologically important properties such as negative differential resistance (NDR) and bistable memory.

We recently described a method[17] to fabricate Au−16-mercaptohexadecanoic acid−Au nanowires using electrochemical template replication, which produced approximately 10^{11} nanowires in each synthetic run. In this paper, we report on the synthesis and electrical transport properties of 30-nm diameter in-wire metal−SAM−metal junctions that incorporate three different molecules: saturated alkane chains of dodecane (C12), π-conjugated oligo(phenylene ethynylene) (OPE), and oligo(phenylene vinylene) (OPV) in dithiolacetates (Figure 1) and three different metal contacts: Au−SAM−Pd, Au−SAM−Ag, and Pd−SAM−Pd. Our previous process was modified to use potential-assisted assembly[23] to enhance molecule diffusion in the template pores, which allowed us to form well-ordered SAMs on the nanowire tips in a shorter amount of time. We also employed new methods for seeding the thiol-terminated SAMs with Ag and Pd nanoparticles before electrodepositing the top metal nanowire segment. Room-temperature current−voltage (I−V) measurements of these molecular junctions show that for a particular pair of metal contacts the conductance of OPV molecular wire junctions are approximately 1 order of magnitude larger than the OPE molecular wire junctions and 3 orders of magnitude larger than the C12 insulating junctions. Current densities obtained for in-wire junctions formed with S−Au contacts are comparable to those measured using a crossing-wire test bed.[19] In addition, junctions formed with symmetric S−Pd contacts had higher conductance than those

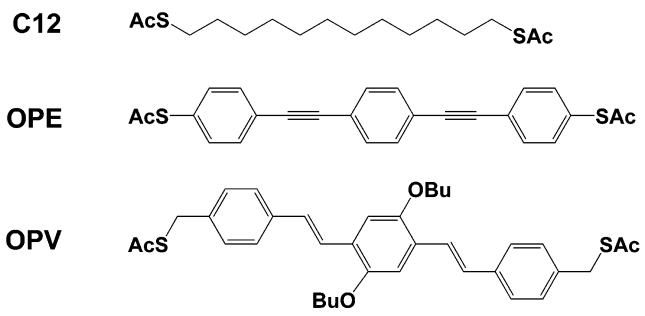

Ac=Acetyl-; Bu=Butyl-

Figure 1. The molecular structures of the C12, OPE, and OPV molecules investigated in this paper.

* Author to whom correspondence may be addressed. Tel: 814-863-8458. Fax: 814-865-7065. E-mail: tsm2@psu.edu.
[†] Department of Electrical Engineering, The Pennsylvania State University.
[‡] Department of Chemistry, The Pennsylvania State University.
[§] Naval Research Laboratory.

10.1021/jp0361273 CCC: $27.50
Published on Web 02/06/2004

formed with asymmetric S−Au/S−Pd or S−Au/S−Ag contacts. This is in good qualitative agreement with theoretical predictions[24] that the S−Pd interface provides a lower barrier for transport than S−Au or S−Ag, which are both similar.

These results demonstrate that in-wire molecular junctions fabricated using template replication may facilitate rapid screening of the electrical properties of metal−molecule−metal devices containing different molecular structures, end-groups, and metal contacts. In addition, these "functional nanowires" may also serve as building blocks for interconnecting molecular device junctions directly into ultrahigh-density electronic circuits through bottom-up directed assembly methods.[25,26]

2. Experimental Section

Chemicals. Polycarbonate track-etched (PCTE) membranes (pore sizes of 0.01 μm, thickness of 6 μm) were purchased from Osmonics Inc. Au, Ag, and Pd electroplating solutions were obtained from Technic Inc. All other chemicals were used as received without further purification. The synthesis of the compounds (Figure 1) has been described elsewhere.[19,27]

Nanowire Preparation. Prior to electrodepositing the metal nanowires, one side of a PCTE membrane was coated with a 20-nm Cr and 120-nm Au thick seed metal by thermal evaporation. The Au surface of the membrane was then placed onto a Ag plate, which served as a cathode during electrodeposition. The electrochemical cell was completed by centering a glass tube terminated in an "O"-ring seal on top of the membrane and securing the assembly together with a clamp. In all cases, a Ag/AgCl electrode was used as the reference electrode and a Pt wire as the counter electrode. The bottom Au nanowire segments were electroplated at a constant potential of −0.9 V (EG&G PAR M273 potentiostat) to a length of approximately 3 μm. The bottom Pd segments were grown by performing cyclic voltammetry in the Pd plating solution between 0 and −0.3 V at a scan rate of 20 mV/s for 5 cycles and then holding the potential constant at −0.3 V for the duration of the growth.

Potential-Assisted SAMs. Planar control samples were prepared using silicon substrates coated with 20-nm Cr and 120-nm Au by thermal evaporation. Prior to molecular assembly, the Au surface was cleaned in $NH_4OH/H_2O_2/H_2O$ (1:1:5) for 15 min, rinsed in DI water, and dried in a N_2 flow. According to protocols developed previously,[23] SAMs were formed at a constant potential of +400 mV (vs Ag/Ag^+/ACN) and 0.1−0.5 mM molecular concentration. The solutions were prepared with a mixed solvent of EtOH/MeOH/acetone (15:1:2) and a supporting electrolyte of 0.5 mM tetrabutylammonium perchlorate (TBAP). Monolayers were assembled directly from the thioacetyls without base/acid deprotection to avoid forming disulfide-linked multilayers. After incubation for 1−6.5 h in an inert atmosphere, the resulting SAMs were deprotected to form free thiol ends with the addition of 0.5% NH_4OH for 5 min. Blocking experiments were performed on samples with electrode areas of 0.45 cm^2 by cyclic voltammetry from −0.2 to +0.6 V at scan rate of 50 mV/s in 1 mM $K_3[Fe(CN)]_6$ and 0.1 M KCl aqueous solutions. The same procedures were used to deposit SAMs on the tips of the Au metal nanowires within the membrane pores.

Nanoparticle Seeding and Top Metal Electrodeposition. Pd nanoparticle seeding was accomplished by first soaking the PCTE membrane in 3 mM $(NH_3)_4PdCl_2/H_2O$ for 12 h to adsorb Pd ions onto the free thiol end of the SAMs. The Pd ions were then electrochemically reduced to Pd nanoparticles in a Pd plating solution by cyclic voltammetry from 0 to −0.3 V (or −0.4 V) at a scan rate of 20 mV/s for 5 cycles, after which the potential was held at −0.3 V (or −0.4 V) for 5−10 min. Similarly, Ag nanoparticle seeding was initiated by soaking the PCTE membrane in 10 mM $AgNO_3$ for 15 min. The Ag ions were then chemically reduced to Ag nanoparticles by immersion in 25 mM $NaBH_4$ for 5 min and development in commercial silver enhancement solution (Sigma, Silver Enhancer Kit) diluted 1:2 with DI water for 1 min. After capping the SAMs with the Pd or Ag seed layers, the top segment of the Au nanowires were electrodeposited by gradually stepping the constant potential from −0.3 V to −0.9 V until the Au segments emerged from the PCTE surface. The residual Au layer was wiped off of the PCTE membranes leaving the nanowires inside the pores.

Nanowire Assembly and I−V Characterization. The nanowires were released from the PCTE membrane by being dissolved in dichloromethane. Electrical characterization was facilitated by electrofluidically aligning individual nanowires between pairs of metal electrodes (5 μm long, 1 μm wide, 3−5 μm gap) that were defined lithographically on an oxidized silicon wafer using procedures published elsewhere.[28] Briefly, alignment took place by dispersing 10 μL of the nanowire suspension onto arrays consisting of 100 metal electrodes that were biased with an alternating voltage of 5 V_{rms} at 10 kHz. The bias was maintained until the dichloromethane evaporated, which typically occurred in less than 1 min. After alignment, I−V measurements of individual metal nanowires and in-wire metal−molecule−metal junctions were carried out at room temperature using an Agilent 4155C semiconductor parameter analyzer. Electrical connections were made using a Micromanipulator 7000 probe station and low-noise coaxial probe holders, permitting measurement of sub-100 fA current levels.

Ellipsometry. The thickness of the SAMs deposited on planar control substrates was determined using a dual-mode automatic ellipsometer L116A (Gaertner Sci. Corp.) with He−Ne laser light (632.8 nm) incident at a 70° incident angle. The thickness was measured based on a refractive index of $n_f = 1.5$, $k_f = 0$. The ideal monolayer thickness was calculated from a molecule length between the dithiol groups using a bond length of 0.24 nm for Au−S bond.

3. Results and Discussion

Metal−SAM−metal nanowires were synthesized by electrochemical template replication in nanopores of a polycarbonate track-etched membrane, which produced nanowires with diameter of 30−40 nm. Template replication[29,30,31] has been used to fabricate large quantities of ($10^{11}/cm^2$) monodisperse nanowires that incorporate different metals or junctions (i.e., semiconductor, conducting polymer, etc.) along the length of the wire. The nanowire diameter is determined by the pore size, and their length is controlled by adjusting the amount of charge passed during electrodeposition at a constant potential. We formed metal−molecule junctions at the tips of nanowires by depositing SAMs of C12, OPE, and OPV molecules using a potential-assisted assembly method, which results in well-ordered SAMs with shorter incubation times. Compared to chemical assembly,[32] where the open circuit potential is approximately −0.5 V (vs Ag/Ag^+/ACN), electrochemical assembly at +0.4 V improves molecule diffusion into the membrane pores and molecule adsorption at the tips of nanowires. SAMs were formed directly from the thioacetyls without base or acid deprotection to prevent multilayer formation due to the oxidative coupling of the terminal thiol groups forming disulfide-bridged species. Moreover, the remaining thioacetyl protected-groups also prevented oxidation of the SAM when exposed in air.

TABLE 1: Potential-Assisted Self-Assembly of C12, OPE, and OPV Molecules on Planar Au or Pd Substrate[a]

molecule	substrate	time	block %	D (exp)	D_0 (calcd)
C12	Au	3.5 h	93%	1.6 ± 0.1 nm	1.63 nm
OPV	Au	6.5 h	98%	2.5 ± 0.1 nm	2.30 nm
OPE	Au	5.0 h	99%	2.4 ± 0.1 nm	2.27 nm
OPE	Pd	5.0 h	93%	2.4 ± 0.2 nm	2.27 nm

[a] The blocking ratio and experimental and calculated values of SAM thickness are provided in the last three columns of the table. The blocking ratio of the SAM is deduced by $(1 - I_{SAM}/I_{Au})\%$ from the redox current of ferricyanide/ferrocyanide solution.

Table 1 compares the experimental and calculated thicknesses and blocking ratio of three different molecular monolayers assembled onto Au and Pd planar control samples. The measured SAM thicknesses were approximately equal to those calculated theoretically, indicating that the potential-assisted assembly method forms a single molecular monolayer rather than a multilayer. The resulting SAMs also show good blockage of a redox reaction of ferrrocyanide/ferricyanide couple, where the oxidation/reduction decreased by more than 93% after SAM adsorption. On the basis of these values for the blocking ratio, we expect that defects in the SAMs (e.g., pinholes) and tip surface roughness would result in fewer than 5−10% of the nanowires with electrically shorted junctions.

The electrical integrity of molecular junctions can be very sensitive to the methods used to form the top metal contact.[11,33] We demonstrated previously[17] that incorporating electroless seed layers formed by sequential reduction of a Sn−Ag−Au nanoparticle multilayer onto carboxylate-terminated SAMs was effective at preventing junction shorting during electrodeposition of the top nanowire segment. However, it was difficult to investigate the properties of the metal−molecule junction due to the complex interfacial coupling between the seed layer and the molecule. Here, we incorporated metal seed layers based on depositing a thin layer of metal nanoparticles (i.e., Ag and Pd) by chemical or electrochemical reduction of metal ions adsorbed onto the free thiol end of the SAM. The nanoparticles serve as a protective layer that minimizes shorting of the molecular junction and as a seed layer to initiate growth of the second nanowire segment at a potential low enough to prevent desorption of the SAM (e.g., less than −0.4V). These procedures simplified the top metal−molecule contact interface and allowed us to study the electrical properties of Au, Ag, and Pd metal contacts to molecules with symmetric thiol end groups.

Nanowires were aligned between pairs of lithographically defined Au electrodes by AC electric-field-assisted assembly.[28] The concentration of nanowires in suspension was adjusted to obtain a high yield of single nanowire alignment. Figure 2 shows scanning electron microscope (SEM) images of a single Au−OPE−Pd nanowire that contacting on a pair of $100 \times 300\ \mu m^2$ metal electrodes used for on-wafer probing. As is evident from these images, the 6 μm long nanowire spans the 3.5 μm wide gap with short segments of the nanowire contacting the left- and right-hand electrodes. Such nanowires are suitable for electrical measurement because the molecular junction is nearly centered in the gap between the two metal electrodes.

Several control experiments were performed before the nanowire molecular junctions were characterized electrically. First, the leakage current was measured between pairs of large area metal electrodes prior to nanowire alignment to verify the quality of the test structure. In all cases, the current was found to be less than 200 fA for voltages of ± 1 V, which is much smaller than the levels of current expected for the molecular junctions studied here. Second, the resistance of the structure

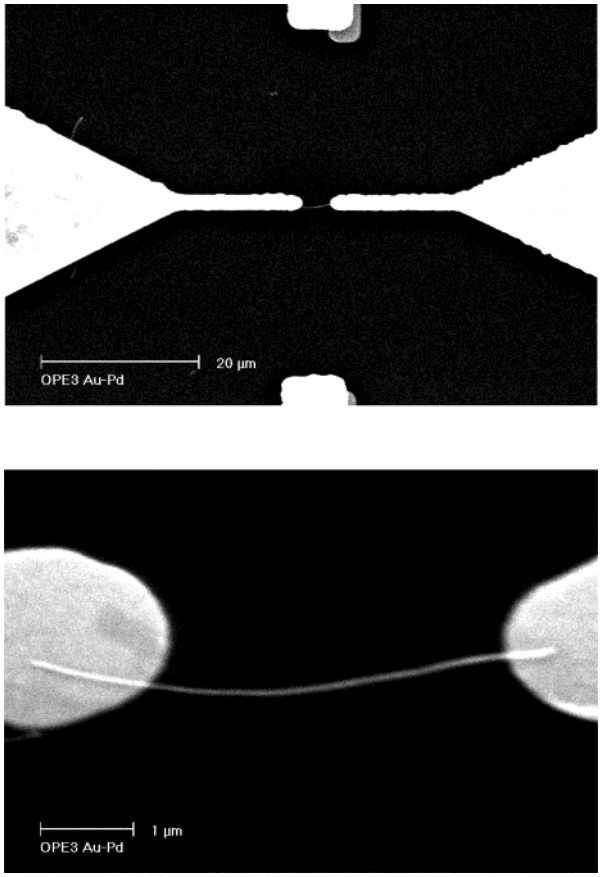

Figure 2. SEM images of a Au−OPE−Pd nanowire contacted at each tip by a pair of Au pads at (a) lower magnification and (b) higher magnification.

following alignment of 30−40 nm diameter solid Au nanowires was determined. Linear I−V properties were observed for all the Au nanowires that were measured, with currents of approximately 50 μA at 10 mV. This results in a total nanowire and contact resistance of approximately 200 Ω, which gives a maximum contact resistance between the metal nanowire and bottom electrode of approximately 70 Ω.[34] This confirmed that contact resistance between the 40 nm diameter Au nanowire and the measurement electrode was negligible compared to the expected resistance due to the molecular junction.

Electrical properties of the molecular nanowire junctions were measured at room temperature for SAMs of C12, OPE, and OPV molecules. Figure 3 shows typical I−V characteristics of Au−SAM−Pd junctions plotted on a semilogarithmic scale. Error bars are included to demonstrate the range of currents measured on 10 or more nanowires prepared in multiple synthetic runs to address the junction-to-junction and run-to-run reproducibility of this method. Despite relatively large error bars, these data indicate that the OPV and OPE molecular wire junctions have much higher conductance than the insulating C12 junctions. In particular, the representative current measured at a bias of 1 V for OPE junctions is 5 μA, while that of the OPV junctions is 20 μA. These values of current are approximately 2 and 3 orders of magnitude larger than the C12 junctions, which are 40 nA at a bias of 1 V. The device-to-device variation that we measure could be due to differences in nanowire diameter and contact area (i.e., number of molecules participating in transport).

The trends in conductance measured in these nanowire junctions of C12 < OPE < OPV are in very good agreement with previous experimental data obtained using crossed-wire test bed junctions and with theoretical analyses of conductance

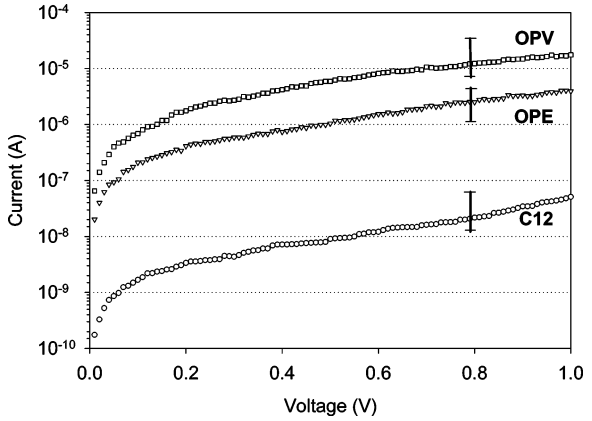

Figure 3. Semilogarithmic I−V characteristics of Au−SAM−Pd junctions formed from C12, OPE, and OPV molecules. Error bars are included for each junction to show the range of currents measured on 10 or more nanowire junctions prepared in multiple synthetic runs.

through alkanes and molecular wires.[19] In accordance with a complete alkanethiol coverage[9] of 9×10^{-10} mol/cm^2 and a molecular structure model with minimized energy, the area occupied by a single molecule is approximately 0.2 nm^2 for C12, 0.28 nm^2 for OPE, and 0.7 nm^2 for OPV. From these values, we estimate that there are approximately 3500, 2500, and 1000 molecules in well-ordered 30 nm diameter C12, OPE, and OPV junctions. Although the exact nature of the junction (i.e., SAM and contacts) is not well understood, our I−V data suggest that the current per OPV molecule at a bias of 1 V is approximately 1 order of magnitude larger than that of the OPE. Theoretical works propose that the higher conductance of OPV as compared to OPE can be attributed to the higher coplanarity of OPV that results in improved π conjugation[35,36] and the shorter bond-length alternation,[19,37] causing a smaller HOMO−LUMO gap for electrical conduction. Electrochemistry measurements[36,38] have also verified that the OPV backbone is a better molecular wire than the OPE backbone.

The zero-bias resistances of our C12 nanowire junctions are approximately $R_0 \approx 6 \times 10^7$ Ω as determined from the slope of the linear segment of the I−V curve between ±10 mV. This corresponds to a resistance per molecule of about 2×10^{11} Ω/molecule that was calculated assuming 3500 C12 molecules per nanowire junction. Values of R_0 have been measured for small bundles of 75 molecules[9] and individual molecules[12] with symmetric Au contacts by CP-AFM and were shown to vary between 8×10^{11} Ω/molecule for C12 monothiols and 8×10^9 Ω/molecule for C12 dithiolates. It has been suggested that dithiolates are more strongly coupled to both the top and bottom contacts through Au−S chemical bonding, which results in lower overall junction resistance.[11] The values of resistance per molecule measured in our asymmetric Au−S−C12−S−Pd nanowire junctions are intermediate between those determined by CP-AFM. Such variations could be expected due to large differences in sample preparation (i.e., electrodeposited vs mechanical top contact) and contact metallurgy (Pd vs Au).

Figure 4 shows the I−V characteristics of the same molecular nanowire junctions on a linear scale (left *y* axis) and the associated molecular conductance (right *y* axis) for biases of ±1 V. There is a notable increase in the conductance gap from approximately 0.2 eV for OPV, 0.7 eV for OPE, and 1.2 eV for C12 molecular junctions, which follows from the differences in the energy gaps of the molecules investigated. In addition, several of the SAM junctions exhibit a slight asymmetry in the conductance gap around 0 V. It is possible that this asymmetry is

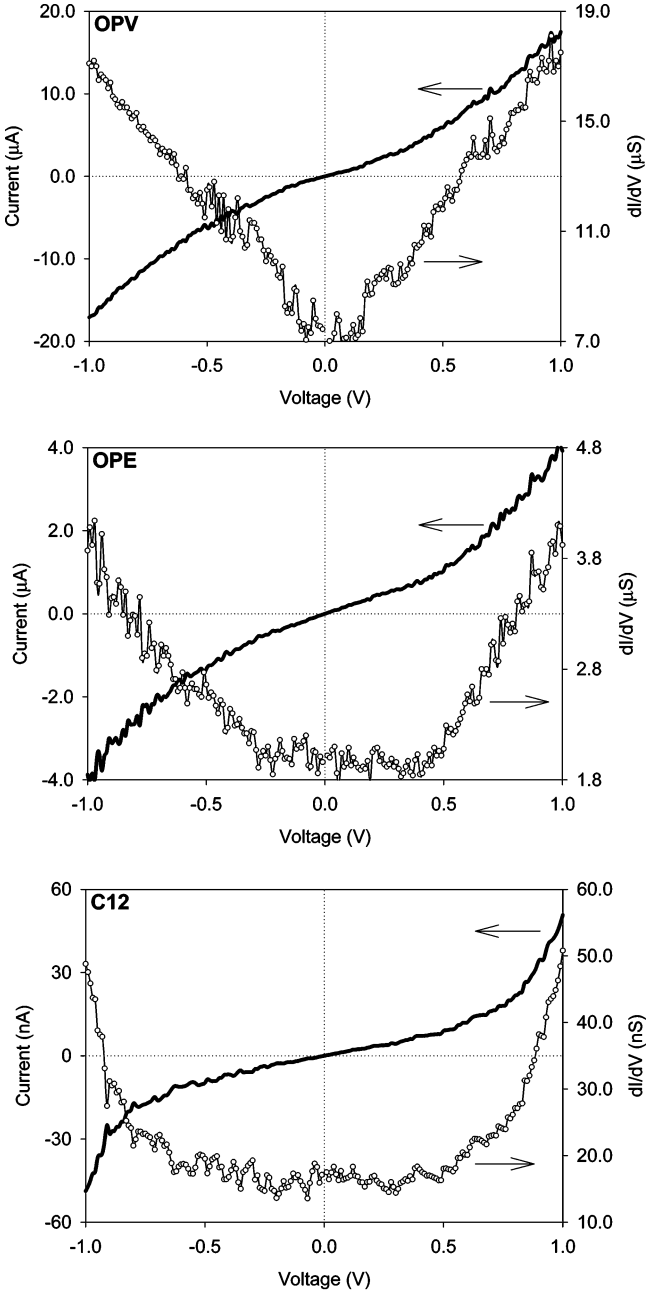

Figure 4. Linear I−V characteristics (left *y* axis) and conductance d*I*/d*V* (right *y* axis) of Au−SAM−Pd junctions shown in Figure 3.

due to the differences in Au and Pd coupling with the thiol end groups of the molecule, which results in different contact barriers.[39]

Conductance through metal−molecule junctions was also found to be dependent on the coupling and contact between metal and molecule.[11,24,39−42] Figure 5 shows I−V characteristics of OPE junctions with three different metal contacts, Au−Ag or Au−Pd and Pd−Pd, plotted on a semilogarithmic scale. Each of these metals is very reactive with the thiol end groups of the OPE and forms a stable metal−S chemical bond. These I−V characteristics show that the typical current at a bias of 1 V of the Au−Ag and Au−Pd junctions is approximately 5 μA, while the current of the junction formed with Pd−Pd contacts is nearly an order of magnitude larger. This confirms that the metal−molecule interface plays a strong role in charge transport in molecule junctions, with the symmetric S−Pd contacts resulting in junctions with the highest conductance.

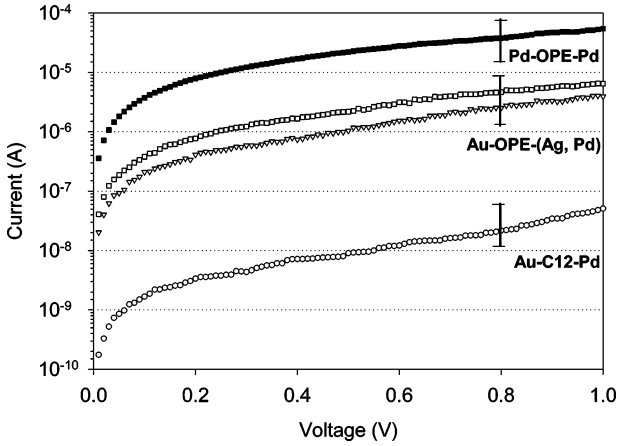

Figure 5. Semilogarithmic I−V characteristics of metal−OPE−metal junctions formed with Au−Ag, Au−Pd, and Pd−Pd metal contacts.

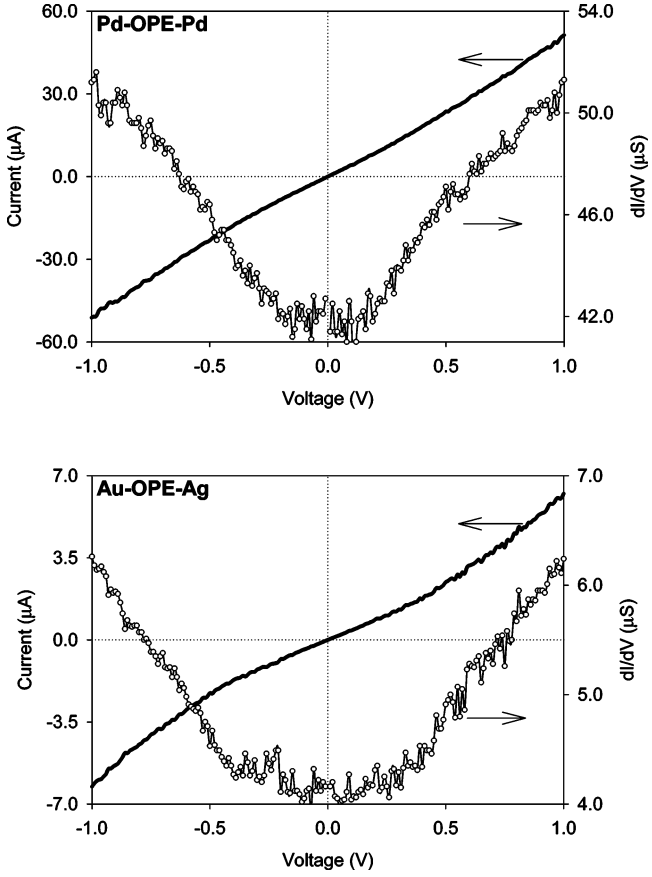

Figure 6. Linear I−V characteristics (left *y* axis) and conductance d*I*/d*V* (right *y* axis) of the Pd−OPE−Pd and Au−OPE−Ag junctions shown in Figure 5.

Corresponding I−V characteristics plotted on a linear scale (left *y* axis) and the associated molecule conductance (right *y* axis) for biases of ±1 V are shown in Figure 6. Here it is noted that the symmetry and width of the conductance gap also depends on the molecule−metal interface. In our nanowires, the gap is approximately 0.7 eV for Au−OPE−Ag junctions, which is nearly equal to that of Au−OPE−Pd junctions (see Figure 4). A smaller gap of 0.4 eV is measured for the Pd−OPE−Pd junctions. The conductance gap is nearly symmetric about 0 V for junctions with Au−Ag and Pd−Pd contacts.

Seminario et al.[24] have investigated theoretically using a Green function approach the conductance of phenyl molecules with symmetric thiol and isonitril end groups contacted by metals including Au, Ag, and Pd. These calculations suggest that the S−Pd contacts will result in junctions with the highest conductance, while the S−Ag and S−Au contacts will have similar and much lower conductances. Similar differences are also noted for NC-based contacts using the same metals. Measurements made using nanopore test beds[42] supported the conclusion that NC−Pd produced junctions with higher conductance than NC−Au contact. The data presented in this paper is also consistent with this theoretical analysis. In particular, lower values of current observed with one or more of the contacts are formed by S−Au or S−Ag bond in comparison to the junctions that contained symmetric S−Pd contacts. Moreover, the asymmetric behavior in the conductance gap of the Au−Pd junction may be due to the larger contact barrier of S−Au limiting electron transport in the Au−OPE−Pd junction.[39]

In conclusion, we have fabricated and characterized the electrical properties of nanowire molecular junctions synthesized in large quantity using electrochemical template replication techniques. We investigated junctions formed using three molecules, C12, OPE, and OPV, and three metal−molecule contacts, Au−Ag, Au−Pd, and Pd−Pd. High quality junctions were made by incorporating potential-assisted self-assembly to produce well-ordered monolayers in a shorter assembly times. Moreover, Ag or Pd nanoparticles were (electro)chemically deposited on top of the thiol-terminated SAMs to serve as a seed metal for growth of the second nanowire segment. We found that π-conjugated dithiol oligomers were very good molecular wires with the OPV molecules having higher conductance than the OPE molecules. The Pd−Pd metal contact resulted in molecular wire junctions with the highest conductance and hence the best electronic coupling to the molecular junction. Such "functional nanowires" fabricated using simple, reproducible methods such as those presented in the paper will facilitate self-assembly of individual molecular devices into large-scale memory and logic circuits.

Acknowledgment. This work was supported by DARPA/ONR under contact No. ONR-N00014-98-1-0846 (Penn State), DARPA (NRL), and NSF MRSEC Center for Nanoscale Science Grant #DMR-008001. The authors wish to acknowledge the Penn State Materials Characterization Laboratory for the use of the microscopy facilities.

References and Notes

(1) Joachim, C.; Gimzewski, J. K.; Aviram, A. *Nature* (London) **2000**, *408*, 541−548.

(2) Andres, R. P.; Bein, T.; Dorogi, M.; Feng, S.; Henderson, J. I.; Kubiak, C. P.; Mahoney, W.; Osifchin, R. G.; Reifenberger, R. *Science* **1996**, *272*, 1323−1325.

(3) Bumm, L. A.; Arnold, J. J.; Cygan, M. T.; Dunbar, T. D.; Burgin, T. P.; Jones, L.; Allara, D. L.; Tour, J. M.; Weiss, P. S. *Science* **1996**, *271*, 1705−1707.

(4) Reed, M. A.; Zhou, C.; Muller, C. J.; Burgin, T. P.; Tour, J. M. *Science* **1997**, *278*, 252−254.

(5) Kergueris, C.; Bourgoin, J. P.; Palacin, S.; Esteve, D.; Urbina, C.; Magoga, M.; Joachim, C. *Phys. Rev. B* **1999**, *59*, 12505−12513.

(6) Reichert, J.; Ochs, R.; Beckmann, D.; Weber, H. B.; Mayor, M.; Löhneysen, H. V. *Phys. Rev. Lett.* **2002**, *88*, 176804-(1−4).

(7) Donhauser, Z. J.; Mantooth, B. A.; Kelly, K. F.; Bumm, L. A.; Monnell, J. D.; Stapleton, J. J.; Price, D. W.; Rawlett, A. M.; Allara, D. L.; Tour, J. M.; Weiss, P. S. *Science* **2001**, *292*, 2303−2307.

(8) Park, J.; Pasupathy, A. N.; Goldsmith, J. I.; Chang, C.; Yaish, Y.; Petta, J. R.; Rinkoski, M.; Sethna, J. P.; Abruna, H. D.; Mceuen, P. L.; Ralph, D. C. *Nature* **2002**, *417*, 722−725.

(9) Wold, D. J.; Frisbie, C. D. *J. Am. Chem. Soc.* **2001**, *123*, 5549−5556.
(10) Wold, D. J.; Haag, R.; Rampi, M. A.; Frisbie, C. D. *J. Phys. Chem. B* **2002**, *106*, 2813−2816.
(11) Cui, X. D.; Primak, A.; Zarate, X.; Tomfohr, J.; Sankey, O. F.; Moore, A. L.; Moore, T. A.; Gust, D.; Harris, G.; Lindsay, S. M. *Science* **2001**, *294*, 571−574.
(12) Cui, X. D.; Primak, A.; Zarate, X.; Tomfohr, J.; Sankey, O. F.; Moore, A. L.; Moore, T. A.; Gust, D.; Nagahara, L. A.; Lindsay, S. M. *J. Phys. Chem. B* **2002**, *106*, 8609−8614.
(13) Haag, R.; Rampi, M. A.; Holmlin, R. E.; Whitesides, G. M. *J. Am. Chem. Soc.* **1999**, *121*, 7895−7906.
(14) Holmlin, R. E.; Haag, R.; Chabinyc, M. L.; Ismagilov, R. F.; Cohen, A. E.; Terfort, A.; Rampi, M. A.; Whitesides, G. M. *J. Am. Chem. Soc.* **2001**, *123*, 5075−5085.
(15) Zhou, C.; Deshpande, M. R.; Reed, M. A.; Jones, L., II; Tour, J. M. *Appl. Phys. Lett.* **1997**, *71*, 611−613.
(16) Chen, J.; Wang, W.; Reed, M. A.; Rawlett, A. M.; Price, D. W.; Tour J. M. *Appl. Phys. Lett.* **2000**, *77*, 1224−1226.
(17) Mbindyo, J. K. N.; Mallouk, T. E.; Mattzela, J. B.; Kratochvilova, I.; Razavi, B.; Jackson, T. N.; Mayer, T. S. *J. Am. Chem. Soc.* **2002**, *124*, 4020−4026.
(18) Collier, C. P.; Wong, E. W.; Belohradsky, M.; Raymo, F. M.; Stoddart, J. F.; Kuekes, P. J.; Williams, R. S.; Heath, J. R. *Science* **1999**, *285*, 391−394.
(19) Kushmerick, J. G.; Holt, D. B.; Pollack, S. K.; Ratner, M. A.; Yang, J. C.; Schull, T. L.; Naciri, J.; Moore, M. H.; Shashidhar, R. *J. Am. Chem. Soc.* **2002**, *124*, 10654−10655.
(20) Chen, J.; Reed, M. A.; Rawlett, A. M.; Tour, J. M. *Science* **1999**, *286*, 1550−1552.
(21) Reed, M. A.; Chen, J.; Rawlett, A. M.; Price, D. W.; Tour, J. M. *Appl. Phys. Lett.* **2001**, *78*, 3735−3737.
(22) Collier, C. P.; Mattersteig, G.; Wong, E. W.; Luo, Y.; Beverly, K.; Sampaio, J.; Raymo, F. M.; Stoddart, J. F.; Heath, J. R. *Science* **2000**, *289*, 1172−1175.
(23) Cai, L.; Yao, Y.; Yang, J.; Price, D. W., Jr.; Tour, J. M. *Chem. Mater.* **2002**, *14*, 2905−2909.
(24) Seminario, J. M.; De La Cruz, C. E.; Derosa, P. A. *J. Am. Chem. Soc.* **2001**, *123*, 5616−5617.
(25) Huang, Y.; Duan, X.; Cui, Y.; Lauhon, L.; Kim, K.; Lieber, C. M. *Science* **2001**, *294*, 1313−1317.
(26) Bachtold, A.; Hadley, P.; Nakanishi, T.; Dekker, C. *Science* **2001**, *294*, 1317−1320.
(27) Tour, J. M.; Rawlett, A. M.; Kozaki, M.; Yao, Y. X.; Jagessar, R. C.; Dirk, S. M.; Price, D. W.; Reed, M. A. *Chem.−Eur. J.* **2001**, *7*, 5118−5134.
(28) Smith, P. A.; Nordquist, C. D.; Jackson, T. N.; Mayer, T. S.; Martin, B. R.; Mbindyo, J. K. N.; Mallouk, T. E. *Appl. Phys. Lett.* **2000**, *77*, 1399−1401.
(29) Martin, C. R. *Science* **1994**, *266*, 1961−1966.
(30) Schonenberger, C.; van der Zande, B. M. I.; Fokkink, L. G. J.; Henny, M.; Schmid, C.; Kruger, M.; Bachtold, A.; Huber, R.; Birk, H.; Staufer, U. *J. Phys. Chem. B* **1997**, *101*, 5497−5505.
(31) Pena, D. J.; Mbindyo, J. K. N.; Carado, A. J.; Mallouk, T. E.; Keating, C. D.; Razavi, B.; Mayer, T. S. *J. Phys. Chem. B* **2002**, *106*, 7485−7462.
(32) Tour, J. M.; Jones, L.; Pearson, D. L.; Lamba, J. J. S.; Burgin, T. P.; Whitesides, G. M.; Allara, D. L.; Parikh, A. N.; Atre, S. *J. Am. Chem. Soc.* **1995**, *117*, 9529−9534.
(33) Fisher, G. L.; Walker, A. V.; Hooper, A. E.; Tighe, T. B.; Bahnck, K. B.; Skriba, H. T.; Reinard, M. D.; Haynie, B. C.; Opila, R. L.; Winograd, N.; Allara, D. L. *J. Am. Chem. Soc.* **2002**, *124*, 5528−5541.
(34) Maximum contact resistance calculated assuming the minimum nanowire resistivity is equal to that of bulk Au (i.e., 2×10^{-6} Ω cm) and $R_{total} = R_{nanowire} + 2R_{contact}$.
(35) Davis, W. B.; Ratner, M. A.; Wasielewski, M. R. *Nature* **1998**, *396*, 60−63.
(36) Dudek, S. P.; Sikes, H. D.; Chidsey, C. E. D. *J. Am. Chem. Soc.* **2001**, *123*, 8033−8038.
(37) Heeger, A. J. *J. Phys. Chem. B* **2001**, *105*, 8475−8491.
(38) Creager, S.; Yu, C. J.; Bamdad, C.; O'Connor, S.; MacLean, T.; Lam, E.; Chong, Y.; Olsen, G. T.; Luo, J.; Gozin, M.; Kayyem, J. F. *J. Am. Chem. Soc.* **1999**, *121*, 1059−1064.
(39) Kushmerick, J. G. et al. *The Proceedings of 6th Engineering Foundation Conference on Molecular-Scale Electronics*; Key West, FL, 2002.
(40) Kushmerick, J. G.; Holt, D. B.; Yang, J. C.; Naciri, J.; Moore, M. H.; Shashidhar, R. *Phys. Rev. Lett.* **2002**, *89*, 086802(1−4).
(41) Beebe, J. M.; Engelkes, V. B.; Miller, L. L.; Frisbie, C. D. *J. Am. Chem. Soc.* **2002**, *124*, 11268−11269.
(42) Chen, J.; Calvet, L. C.; Reed, M. A.; Carr, D. W.; Grubisha, D. S.; Bennett, D. W. *Chem. Phys. Lett.* **1999**, *313*, 741−748.